Development 137, 3427-3437 (2010) doi:10.1242/dev.049858
© 2010. Published by The Company of Biologists Ltd

Generation of distinct signaling modes via diversification of the Egfr ligand-processing cassette

Tal Rousso[1], Jeremy Lynch[2], Shaul Yogev[1], Siegfried Roth[2], Eyal D. Schejter[1] and Ben-Zion Shilo[1,*]

SUMMARY

Egfr ligand processing in *Drosophila* involves trafficking of the ligand precursor by the chaperone Star from the endoplasmic reticulum (ER) to a secretory compartment, where the precursor is cleaved by the intramembrane protease Rhomboid. Some of the *Drosophila* Rhomboids also reside in the ER, where they attenuate signaling by premature cleavage of Star. The genome of the flour beetle *Tribolium castaneum* contains a single gene for each of the ligand-processing components, providing an opportunity to assess the regulation and impact of a simplified ligand-processing cassette. We find that the central features of ligand retention, trafficking by the chaperone and cleavage by Rhomboid have been conserved. The single Rhomboid is localized to both ER and secretory compartments. However, we show that *Tribolium* Star is refractive to Rhomboid cleavage. Consequently, this ligand-processing system effectively mediates long-range Egfr activation in the *Tribolium* embryonic ventral ectoderm, despite ER localization of Rhomboid. Diversification of the Egfr signaling pathway appears to have coupled gene duplication events with modulation of the biochemical properties and subcellular localization patterns of Rhomboid proteases and their substrates.

KEY WORDS: Egfr, Ligand processing, TGFα, Rhomboid, Star, *Drosophila*, *Tribolium*, Evolution

INTRODUCTION

The Epidermal growth factor receptor (Egfr) pathway in *Drosophila* triggers a wide range of cellular responses depending on the tissue context, including determination of cell fates, cell proliferation and protection from apoptosis (Shilo, 2003; Shilo, 2005). A variety of molecular mechanisms are employed to regulate activation of the broadly expressed receptor. The level and range of Egfr activation are modulated by inducible negative feedback mechanisms (Casci et al., 1999; Ghiglione et al., 2003; Golembo et al., 1996b; Kramer et al., 1999; Reich et al., 1999), whereas the restricted production of active ligands dictates the time and place of pathway activation. Key to this is an intricate ligand-processing mechanism, in which intracellular compartmentalization and trafficking play major roles (Blobel et al., 2009; Shilo, 2005).

The TGFα homolog Spitz (Spi) serves as the cardinal Egfr ligand in *Drosophila*. Generation of an active Spi ligand is achieved by cleavage of the inactive transmembrane Spi precursor (mSpi) by members of the Rhomboid (Rho) family of seven transmembrane domain intramembrane proteases (Urban et al., 2001). Cleavage takes place in a late secretory compartment, to which mSpi, an endoplasmic reticulum (ER) resident protein, is trafficked by the type II single transmembrane domain protein Star (Lee et al., 2001; Tsruya et al., 2002). Rho proteases regulate the sites of Egfr pathway activation by several means. First, since Spi, the chaperone Star and Egfr are all broadly expressed, it is the dynamic and restricted expression patterns of the Rho proteases that determine the spatial and temporal pattern of ligand processing and, consequently, of Egfr activation (Golembo et al., 1996a).

A second tier of regulation is provided by distinct subcellular localization patterns of the proteases. The Rho proteins in *Drosophila* display different intracellular compartment localizations, generating two distinct modes of signaling. Rho-1 (Rhomboid – FlyBase), the major Egfr-related Rho protease, is localized exclusively to the secretory compartment. mSpi molecules that are trafficked to this compartment by Star are efficiently cleaved and released, giving rise to relatively high levels of ligand release and subsequent Egfr activation. By contrast, Rho-2 and Rho-3 (Stet and Roughoid, respectively – FlyBase), which are expressed and active in more restricted settings (Guichard et al., 2000; Schulz et al., 2002; Wasserman et al., 2000), are targeted to both the ER and the secretory compartment (Yogev et al., 2008). We have shown that this additional localization in the ER attenuates the amount of ligand that is processed and secreted. Both ligand and chaperone first encounter Rho proteases of this class in the ER, and a substantial portion is cleaved within this compartment. The cleaved ligand is retained in the ER (Schlesinger et al., 2004). Cleavage of Star is a functionally significant outcome, as the chaperone is inactivated before it has transported the ligand out of the ER. Thus, only a small fraction of the Star molecules remain intact and, as a consequence, these can traffic only a limited amount of ligand precursor to the late compartment, where productive cleavage takes place (Yogev et al., 2008). Taken together, in contrast to the strong activation provided by Rho-1, utilization of the ER-active proteases Rho-2 or Rho-3 gives rise to a restricted signal that can provide only short-range Egfr activation.

Utilization of multiple Rho family proteases that possess distinct expression patterns and subcellular localizations serves as the primary means for regulating Egfr pathway activation levels in *Drosophila*. The complexities associated with this scenario raise the question of how the ligand-processing machinery of this ubiquitous signaling pathway is fashioned in simpler systems. An opportunity to address this issue is provided by the flour beetle *Tribolium castaneum*, for which complete genome sequencing has

[1]Department of Molecular Genetics, Weizmann Institute of Science, Rehovot 76100, Israel. [2]Institute of Developmental Biology, University of Cologne, D-50923 Cologne, Germany.

*Author for correspondence (benny.shilo@weizmann.ac.il)

Accepted 2 August 2010

identified only a single Egfr-associated Rho protease gene, as well as single *spi* and *Star* homologs (Richards et al., 2008). We find that the single *Tribolium* Rho (Tc-Rho) is similar to *Drosophila* Rho-2 and Rho-3 in terms of its localization to both ER and secretory compartments and its ability to trigger only a restricted level of Egfr activation. Surprisingly, although *Tribolium* Star (Tc-Star) preserves the ability to traffic the ligand, it is not cleaved by Rho proteases. Examination of the Star protein of a more anciently diverged species, the wasp *Nasonia*, demonstrated a similar behavior. Domain swaps between *Drosophila* and *Tribolium* Star revealed that the basis for *Drosophila* Star cleavability by Rho proteases lies in its extracellular, rather than transmembrane, domain, consistent either with cleavage of Star outside of the transmembrane domain or with an intermolecular interaction between Star and Rho that is required to mediate Star cleavage. Thus, although Tc-Rho resides in the ER, the refractivity of Tc-Star to cleavage facilitates long-range Egfr signaling. Ligand processing emanating from the midline of *Tribolium* was indeed shown to give rise to MAPK activation in several rows along the adjacent ventral ectoderm.

Our analysis, comparing the Egfr ligand-processing machineries of *Drosophila* and *Tribolium*, highlights the modulation of protein interactions, substrate specificity and differential compartmentalization as a means of diversifying the signaling capacity of signal transduction pathways.

MATERIALS AND METHODS

DNA constructs

For cloning cDNAs of EGF ligand and processing components from other insects, potential orthologs were identified by BLAST searching genome sequence databases of *N. vitripennis* and *T. castaneum* and identifying predicted peptide sequences. The 5′ and 3′ ends were confirmed by RACE PCR using the SMART RACE Kit (Clontech) following the manufacturer's instructions. Only in the case of *Tc-tgfα* was the predicted protein sequence significantly incorrect, and the corrected mRNA sequence was submitted to GenBank under accession GU475090. In addition, since the laboratory strain of *T. castaneum* differs from that used for genome sequencing, the sequences of the other genes are slightly different and were submitted under accession numbers GU475090 (*Tc-star*), GU475092 (*Tc-rho*) and GU475094 (*Nv-star*).

The following constructs were made by subcloning into pUAST-based vectors using the Gateway cloning system (Invitrogen). Tc-Rho, Tc-Rho-GFP (used in Figs S3 and S5 in the supplementary material), Tc-Star-HA (used in Figs 1, 3), Tc-TGFα-HA and Tc-TGFα-Myc were constructed by cloning the appropriate cDNAs into pTGW, pTWG, pTWH or pTWM, respectively (T. Murphy, Carnegie Institute, Washington, USA). Tc-Star-HA and Dm-Star-HA (Tsruya et al., 2007) were tagged with a KDEL sequence at their C-termini by PCR using primers encoding KDEL sequence, and inserted into pUAST-attB or pUAST, respectively.

Tc-Rho was tagged at its C-terminus with a KDEL-encoding sequence by PCR to create Tc-Rho-KDEL, and inserted into pUAST-attB containing a GFP N-terminal fusion.

Nv-Star-HA, Tc-Star-HA (used in Figs 4, 5 and Fig. S3 in the supplementary material) and Dm-Star-HA (used in Figs 4, 5 and Fig. S3 in the supplementary material) were constructed by cloning the appropriate cDNAs into pUAST-attB using *Eco*RI and *Xba*I sites. A triple HA tag was inserted into the *Xba*I site of the vector.

All domain swap constructs in Fig. 5 were made by PCR overlap extension, and were inserted into pUAST-attB containing a triple HA tag.

The TM domain swaps Dm-Star-TcTM and Tc-Star-DmTM were made by exchanging Dm-Star nucleotides 832-918 (residues R278-I306) with Tc-Star nucleotides 154-240 (residues R52-M80).

The N-terminal swaps Dm-N′-Tc-C′-Star and Tc-N′-Dm-C′-Star were generated by exchanging Dm-Star nucleotides 1-831 (residues M1-Y277) with Tc-Star nucleotides 1-153 (residues M1-I51).

The C-terminal swaps Tc-N′+TM-Dm-C′-Star and Dm-N′+TM-Tc-C′-Star were generated by exchanging Dm-Star nucleotides 919-1791 (residues R307-P597) with Tc-Star nucleotides 241-972 (residues R81-I324).

Dm-Star-EigerTM was generated by replacing the TM domain of Star (residues P282-R307) with the TM domain of the type II protein Eiger (residues L37-T62) and insertion into the pUAST vector.

The GlpG construct was amplified by PCR from *E. coli* strain DH5α genomic DNA with specific primers and cloned into pUAST.

The tagged rhomboid constructs Rho-1-GFP, Rho-1-HA-KDEL and Rho-2-GFP have been described previously (Yogev et al., 2008). Rho-1-GFP (Yogev et al., 2008) was converted to Rho-1-RFP using the Gateway system and the pTWR vector. Dm-Star-HA (used in Figs 1, 3 and in Fig. S2 in the supplementary material) (Tsruya et al., 2007), Bm-Star-HA (Tsruya et al., 2002), mSpi-GFP-HA (Yogev et al., 2008) and mSpi-GFP (Schlesinger et al., 2004) have been described previously.

Fly strains

The following lines were used: *MS1096-Gal4*, *GMR-Gal4*, *ey-Gal4,GMR-Gal4*. *UAS-rho-1-HA* and *UAS-Dm-Star* were described previously (Yogev et al., 2008; Tsruya et al., 2002), *UAS-Tc-rho-GFP* was generated by standard P-element transformation protocols, *UAS-Tc-star-HA/UAS-Dm-Star-HA* and *UAS-Tc-rho-KDEL* were generated by phi31 germline transformation into the attP2 and attP18 lines, respectively (Markstein et al., 2008), by Genetic Services.

Cell culture and western blots

Typically, 5×10^6 *Drosophila* S2 cells were transiently transfected using ESCORT-IV (Sigma). Expression of UAS-based vectors was achieved by co-transfection of an *actin-Gal4* plasmid. Cells were harvested 72-96 hours after transfection and lysed in PLB buffer [10 mM NaH_2PO_4+$NaHPO_4$ pH 7.5, 100 mM NaCl, 1% Triton X-100, 0.1% SDS, 0.5% sodium deoxycholate (DOC), 5 mM EDTA] mixed with Complete Protein Inhibitor Cocktail (Roche). Equal amounts of protein (140 μg) were loaded onto SDS-PAGE gels. For Star cleavage assays, 24 hours following transfection, cells were transferred to a serum-free medium, which was collected after an additional 72 hours and loaded onto SDS-PAGE gels. The medium was also concentrated on Centricon Ultra filters (molecular weight cut-off 10,000 Da; Amicon) before loading onto SDS-PAGE gels (shown only for the Bm-Star cleavage).

Antibodies used for western blotting were anti-HA (rabbit 1:1000; Sigma), anti-Actin (mouse 1:200; Sigma), anti-Myc (mouse 1:1000; Santa Cruz) and anti-GFP (chicken 1:5000; Aves).

For cell staining, *Drosophila* S_2R^+ cells were transfected using ESCORT-IV and fixed with 4% paraformaldehyde (PFA) after 48 hours.

Immunohistochemistry

Primary antibodies used were anti-HA (rabbit 1:100; Santa Cruz), anti-GFP for cell staining (chicken 1:1000; Aves), anti-GFP for imaginal disc staining (chicken 1:500; Abcam), anti-Myc (mouse 1:100; Santa Cruz), anti-FasIII (mouse 1:20) and anti-Elav (rat 1:1500; Developmental Studies Hybridoma Bank). Cy2-, Cy3- and Cy5-conjugated secondary antibodies (1:200; Jackson ImmunoResearch) were used.

Staining for all antigens was after fixation in 4% PFA and washes with 0.1% Triton X-100 for eye imaginal discs or PBS for cells.

Stained preparations were mounted in 80% glycerol (imaginal discs) or Immuno-Mount (cells) followed by confocal microscopy analysis.

In situ hybridization and immunohistochemistry in *Tribolium*

Single-color in situ hybridizations were performed using standard techniques (Tautz and Pfeifle, 1989) using digoxigenin-labeled probes, alkaline phosphatase-linked anti-digoxigenin antibody (Roche) at 1:2500 and the NBT/BCIP detection solution (Roche). Simultaneous fluorescent in situ hybridization/immunohistochemistry was performed using the single in situ protocol with the addition of mouse anti-dpERK antibody [generated from ascites fluid of clone MAPK-YT (Sigma M-8159)] at 1:1000 and detection with POD-linked anti-mouse antibody (Invitrogen) at 1:100. The green signal was produced using the Alexa Fluor 488 TSA Kit (Invitrogen)

following the manufacturer's instructions. The red signal was produced using the Fast Red/HNPP Detection Kit using the modified protocol described by Mazzoni et al. (Mazzoni et al., 2008).

RESULTS

A minimal, conserved Egfr ligand-processing machinery in *Tribolium*

Complete genome analysis of *Tribolium castaneum* has revealed a minimal ligand-processing cassette that comprises a single member of each component, i.e. the ligand (Tc-TGFα), chaperone (Tc-Star) and protease (Tc-Rho) (see Fig. S1 in the supplementary material). The simplicity of the *Tribolium* ligand-processing cassette offers the opportunity to gain insight into the ancestral mechanism and to obtain an evolutionary perspective on the events that have shaped the more elaborate ligand-processing system found in *Drosophila*.

We set out to characterize the basic Egfr ligand-processing machinery of *Tribolium* in light of the established features of the *Drosophila* system. cDNA clones spanning the entire coding regions of the constituent *Tribolium* elements were obtained for use in these studies. An initial goal was to determine whether Tc-TGFα serves as a substrate for Rhomboid proteases. We utilized the *Drosophila* S2 cell culture system, which has been extensively used for this assay (Lee et al., 2001; Tsruya et al., 2002). When expressed in S2 cells, Tc-TGFα tagged with the HA epitope at its C-terminus migrated on gels as a ~33 kDa band. Co-transfection with *Drosophila* Rho-1 and Star (Dm-Star) resulted in the appearance of a ~18 kDa HA-tagged form, in parallel to the disappearance of the ~33 kDa precursor band (Fig. 1A,B). This observation is consistent with cleavage in the transmembrane domain of Tc-TGFα and furthermore implies that cleavage occurs following trafficking of the precursor to the secretory compartment, where Rho-1 resides. Rho-1-KDEL, which is targeted to the ER, readily cleaved Tc-TGFα in the absence of Star, indicating that, similar to mSpi, Tc-TGFα can also be cleaved in the ER (Yogev et al., 2008). Importantly, efficient cleavage of Tc-TGFα was also obtained using Tc-Rho (Fig. 1B), implying conservation of this basic feature of active Egfr ligand generation in *Tribolium*. The subcellular site of this cleavage is addressed below.

In *Drosophila*, compartmentalization of the precursor form of the ligand, mSpi, and its intracellular trafficking by Star, are key regulators of signaling. Tight retention of the ligand in the ER ensures its segregation from the compartment where the protease resides and processing takes place. In order to determine whether the *Tribolium* signaling system also utilizes these properties as a means of regulation, we monitored the localization of tagged versions of Tc-TGFα and Tc-Star following expression in cultured *Drosophila* S_2R^+ cells. Similar to *Drosophila* mSpi, Tc-TGFα-Myc was mainly retained in the ER (Fig. 1C,E). Furthermore, when expressed together with either *Tribolium* or *Drosophila* Star, the subcellular distribution of Tc-TGFα was altered significantly, as it was trafficked to a secretory compartment, marked by punctuate staining and colocalization with Rho-1-GFP (Fig. 1D,F). In the reciprocal experiment, co-expression of *Drosophila* mSpi-GFP with Tc-Star resulted in efficient trafficking of mSpi-GFP, as demonstrated by the dramatic change in its subcellular localization from the ER to the secretory compartment (Fig. 1G,H).

Accordingly, and as shown for Dm-Star (Fig. 1I) (Tsruya et al., 2002), Tc-Star was found in both the peri-nuclear ER and the secretory compartment (Fig. 1J); its secretory compartment localization was more prominent than that of Dm-Star. The *Tribolium* Egfr ligand and its chaperone therefore display localization patterns and functional attributes that are similar to those of their *Drosophila* counterparts. Finally, we followed Tc-Star distribution and activity in vivo, in the *Drosophila* eye. When expressed in eye discs, Tc-Star-HA was found predominantly in the ER, in a similar manner to Dm-Star-HA, and in some apical puncta (Fig. 1K,L). From a functional standpoint, expression of Tc-Star in eye discs under the control of *GMR-Gal4* rescued the rough-eye phenotype that results from *Star* haploinsufficiency in adult *Drosophila* eyes, demonstrating the conserved biological activity exhibited by this construct (Fig. 1M-O). Taken together, the basic features of ligand precursor ER retention, trafficking by Star and cleavage by Rhomboid are conserved between *Tribolium* and *Drosophila*.

Tc-Rho displays a dual compartment distribution and activity

Sequence alignment analyses (see Fig. S1 in the supplementary material) reveal that out of the three *Drosophila* Egfr-related Rhomboids, Tc-Rho is most similar to Rho-2, which has been shown to reside and be active in both the ER and secretory compartment (Yogev et al., 2008). To define the intracellular localization of Tc-Rho and the site of its activity, a cDNA for Tc-Rho was fused at the C-terminus to GFP and used for the generation of transgenic flies. Expression of Tc-Rho-GFP in *Drosophila* eye discs revealed an ER peri-nuclear distribution, in addition to punctate structures that colocalized with Rho-1 (Fig. 2A,B). Co-expression of mSpi and Tc-Rho in S2 cells in the absence of Star provides an assay for ER cleavage potency. Significant cleavage activity in the ER was detected for Tc-Rho using this approach (see Fig. S2 in the supplementary material).

We next used the *Drosophila* wing imaginal disc to assess functional aspects of Tc-Rho activity in vivo. In this tissue, the Egfr pathway patterns wing veins, following the restricted expression of Rho-1 (Sturtevant et al., 1993). Consequently, ectopic expression of Rho-1 in the wing disc led to ectopic vein structures in the adult wing (Fig. 2C,D). Significantly milder expansion of vein structures was observed following ectopic expression of Rhomboids that are also active in the ER, indicating attenuation of Egfr signaling (Yogev et al., 2008). Ectopic expression of Tc-Rho in the wing disc caused a mild vein phenotype indicative of low levels of released ligand, suggesting that the attenuating activity in the ER is associated with this protease (Fig. 2E).

The attenuated signal mediated by Rhomboids that cleave in the ER has been shown to result primarily from cleavage of Star in the ER, which leads to its inactivation, and is thus highly sensitive to Star dosage (Yogev et al., 2008). Accordingly, the mild wing vein phenotype generated by expression of Tc-Rho was attenuated by removing one allele of *Star* and was significantly enhanced upon co-expression of Dm-Star or Tc-Star with Tc-Rho (Fig. 2F-I). Star overexpression uncovers the activity of Tc-Rho in the ER, as it allows trafficking and secretion of cleaved ligand that was generated in the ER. When testing a Tc-Rho-KDEL construct, which is exclusively targeted to the ER, similar results were obtained, with a strong Egfr hyperactivation phenotype upon co-expression of Star (Fig. 2J-L). Thus, the low level of Egfr signaling elicited by Tc-Rho can be attributed to its ER localization.

Taken together, these observations demonstrate that, when expressed in *Drosophila*, Tc-Rho displays the functional hallmarks of fly ER-active Rhomboids, i.e. a capacity to cleave substrates in the ER as well as in the late compartment and the generation of a Star-dependent, attenuated Spi signal.

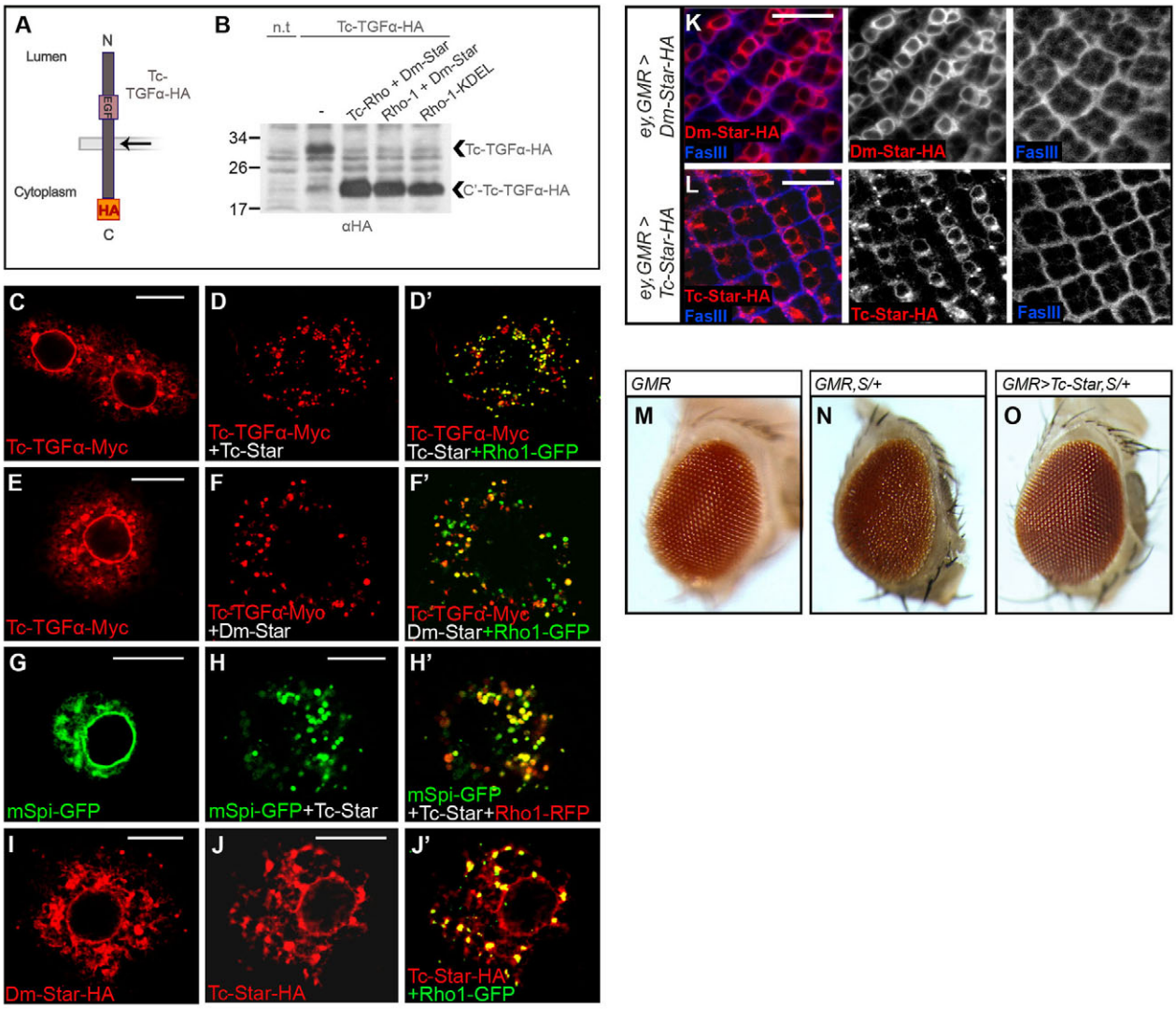

Fig. 1. Conservation of the basic ligand-processing cassette between *Tribolium* and *Drosophila*. (**A**,**B**) Tc-TGFα is cleaved by *Tribolium* and *Drosophila* Rhomboids. (A) Schematic of the C-terminally HA-tagged Tc-TGFα construct positioned relative to the cell membrane. Arrow indicates the presumed site of cleavage by Rhomboids. (B) Tc-TGFα-HA was co-expressed in *Drosophila* S2 cells with the indicated constructs, and cell lysates were probed with an anti-HA antibody. In the presence of Tc-Rho or Rho-1 and Dm-Star, the cleaved C-terminal form of Tc-TGFα was detected at ~18 kDa, parallel to the disappearance of the precursor at ~33 kDa. Tc-TGFα was also cleaved by Rho-1-KDEL in the absence of Star, indicating cleavage in the endoplasmic reticulum (ER). n.t, non-transfected. (**C-J'**) The components of the *Tribolium* and *Drosophila* ligand-processing machinery were localized in *Drosophila* S_2R^+ cells. (C-F) Tc-TGFα-Myc is mainly retained in the ring-like peri-nuclear ER (C,E), and is trafficked by Tc-Star (D) or Dm-Star (F) to the secretory compartment as indicated by colocalization with Rho-1-GFP (D′,F′). (G,H) Tc-Star traffics mSpi from the ER (G) to the secretory compartment (H,H′). (I,J) Tc-Star-HA shows ER localization, as indicated by the peri-nuclear ring (J), combined with secretory compartment localization indicated by colocalization with Rho-1-GFP (J′). Dm-Star-HA is found in similar locations, but resides mainly in the ER (I). (**K**,**L**) Expression of Tc-Star-HA and Dm-Star-HA in eye discs under the control of *ey-Gal4,GMR-Gal4*. Similar to Dm-Star (K), Tc-Star is found predominantly in the peri-nuclear ER and also in apical puncta (L). (**M-O**) Tc-Star rescues the *Star* haploinsufficiency phenotype in the eye when expressed under the control of *GMR-Gal4*. Scale bars: 10 μm.

Tc-Star is not cleaved by Rhomboids

Dm-Star cleavage in the ER by ER-active Rhomboids is one of the main modulators of *Drosophila* Egfr signaling, as it limits the amount of intact Dm-Star that is capable of trafficking the Spi ligand to the secretory compartment, where it is cleaved and secreted. Given the close functional correspondence between Tc-Rho and the *Drosophila* ER-active Rhomboids, we sought to determine whether Star cleavage can also play a role in the regulation of the *Tribolium* signaling system.

We compared the ability of Tc-Star and Dm-Star to be cleaved by different Rhomboids in *Drosophila* S2 cells. Star cleavage by Rhomboids was previously demonstrated in heterologous systems such as COS cells (Tsruya et al., 2007) and is therefore unlikely to require species-specific auxiliary proteins. We co-expressed C-terminally HA-tagged versions of the two Star proteins with different Rhomboid proteins that are localized to distinct intracellular compartments. These included Tc-Rho, Rho-1-KDEL, which is targeted to the ER, and Rho-1, which resides in the

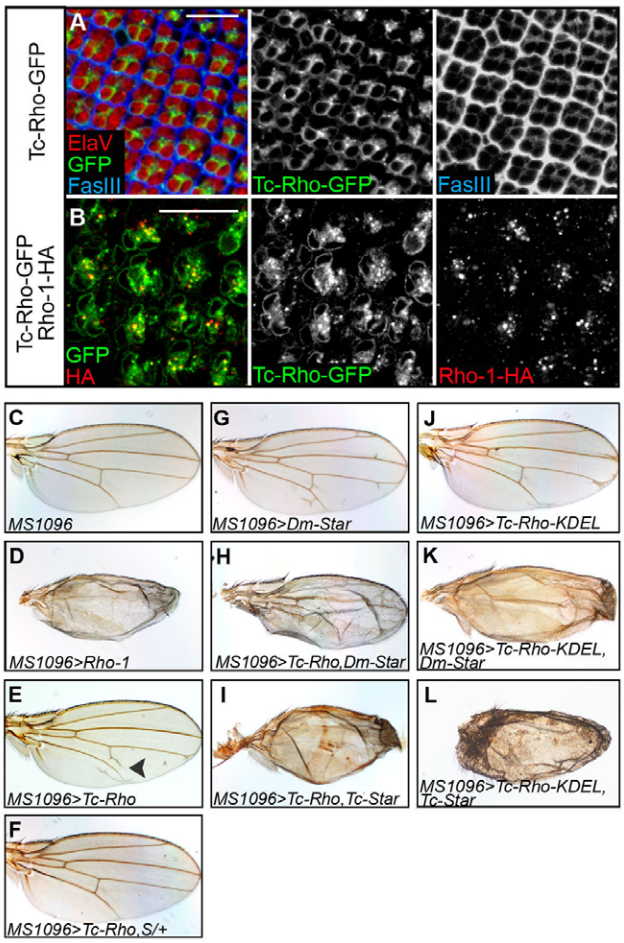

Fig. 2. Tc-Rho is localized in a dual ER and secretory compartment distribution and elicits an attenuated signal. (**A**,**B**) Tc-Rho-GFP displays combined ER and secretory compartment localization when expressed in *Drosophila* eye discs under *ey-Gal4,GMR-Gal4*, which was used to drive expression of the indicated constructs. The GFP tag is detected in the peri-nuclear ER, as a ring surrounding the photoreceptor nuclei (Elav, red) and in cytoplasmic puncta (A). FasIII marks the plasma membrane. An apical focal plane of the eye disc reveals colocalization with Rho-1-HA at the punctate structures, indicating a secretory compartment distribution of Tc-Rho, in addition to the ER (B). (**C-E**) Tc-Rho elicits attenuated Egfr activation in the wing, which is sensitive to the levels of Star. *MS1096-Gal4*, driving expression of the indicated constructs, was examined in heterozygous female wings. (C) Wild-type wing. (D) Rho-1 expression leads to a very pronounced Egfr hyperactivation phenotype, reflected in ectopic vein structures. (E) Expression of Tc-Rho leads to a mild ectopic vein phenotype (arrowhead), suggesting ER activity. (**F-I**) Tc-Rho activity shows high sensitivity to the levels of Star. The Tc-Rho ectopic vein phenotype is suppressed upon removing one allele of *Star* (F) and becomes significantly enhanced upon overexpression of Dm-Star (H) or Tc-Star (I). Expression of Dm-Star alone gives rise to only a mild vein phenotype (G); Tc-Star alone behaved similarly (not shown). (**J**) A very mild vein phenotype is elicited by the expression of Tc-Rho-KDEL. (**K**,**L**) Upon co-expression of Dm-Star (K) or Tc-Star (L) at high levels, the cleaved Spi is trafficked out of the ER, giving rise to a strong vein phenotype, thus underscoring the ER cleavage activity of Tc-Rho. D,H,I,K,L are shown at 1.25× relative to C,E,F,G,J. Scale bars: 10 μm.

secretory compartment and has been extensively analyzed for its ability to cleave Dm-Star (Tsruya et al., 2007). Strikingly, whereas co-expression of Dm-Star with the different Rhomboids resulted in the appearance of a ~30 kDa cleavage fragment, no such cleavage was observed following co-expression of Tc-Star with any of the Rhomboids, neither within the cells, nor by using a more sensitive assay that monitored the cleaved form secreted into the medium (Fig. 3B). Addition of Egfr ligands (mSpi or Tc-TGFα), thereby mimicking the physiological scenario more closely, did not alter these observations (see Fig. S3 in the supplementary material).

To ensure that the inability of Rhomboids to cleave Tc-Star did not result from distinct subcellular localizations, we used KDEL-tagged versions of both Star and Rhomboid proteins for simultaneous targeting to the ER. Whereas Dm-Star was efficiently cleaved by both the *Drosophila* and *Tribolium* Rhomboids, Tc-Star remained uncleaved (Fig. 3C). Thus, it appears that unlike Dm-Star, Tc-Star is not susceptible to cleavage by any of the Rhomboid variants analyzed here.

The observation that Tc-Rho possesses the ability to cleave Dm-Star suggests that the difference in Star cleavability between the two species represents an intrinsic feature of Tc-Star, rather than functional diversity of Tc-Rho. To further investigate this notion under extreme conditions, we examined the competence of the bacterial Rhomboid GlpG to cleave the different Star proteins. Interestingly, GlpG cleaved Dm-Star very efficiently (Fig. 3D), demonstrating that the capacity of Rhomboids to recognize and cleave Star is exceptionally well conserved. GlpG could not cleave Tc-Star (Fig. 3D), further indicating that the difference in Star cleavage capacity derives from diversity in Star cleavability rather than in the activity of Rhomboids.

Divergence of Star cleavability by Rhomboids during insect evolution

To address the divergence in Star cleavability during evolution we examined the Star proteins of different insect species for the capacity to be cleaved by Rhomboids in S2 cells. Star proteins show considerable sequence divergence in different insect species (see Fig. S1D in the supplementary material). We first chose the wasp *Nasonia vitripennis* as a representative of the Hymenoptera, the most basally branching Holometabolous insect order, which shared its most recent common ancestor with *Drosophila* and *Tribolium* ~350 million years ago (Wiegmann et al., 2009). cDNAs of *Star* from *Nasonia* (*Nv-star*), *Tribolium* and *Drosophila* were cloned into the same vector containing a triple HA tag, in order to compare cleavage competence under the same expression conditions. When expressed in *Drosophila* S_2R^+ cells, the different Star proteins displayed both ER and secretory compartment localization (see Fig. S4 in the supplementary material). Nv-Star remained uncleaved when expressed with different Rhomboid proteins from different species, as only the full-length form of ~53 kDa could be detected in the cells, in addition to a Rhomboid-independent cleavage form in the medium (Fig. 4A; see Fig. S4 in the supplementary material). This demonstration that the Star homolog of a more basally branching insect species is refractory to cleavage by Rhomboid proteases supports the idea that Star homologs were ancestrally uncleavable by Rhomboids, and that Rhomboid-mediated cleavage of Star proteins is a derived situation that originated after the divergence of the lineages leading to *Tribolium* and *Drosophila*.

To better define the evolutionary time point at which Star obtained cleavability, we examined the Star protein of the silkworm *Bombyx mori* (Lepidoptera) (Bm-Star), which shared a common ancestor with *Drosophila* ~20 million years more recently than *Tribolium* (Wiegmann et al., 2009). Interestingly, when Bm-Star was HA tagged C-terminally and co-expressed with different

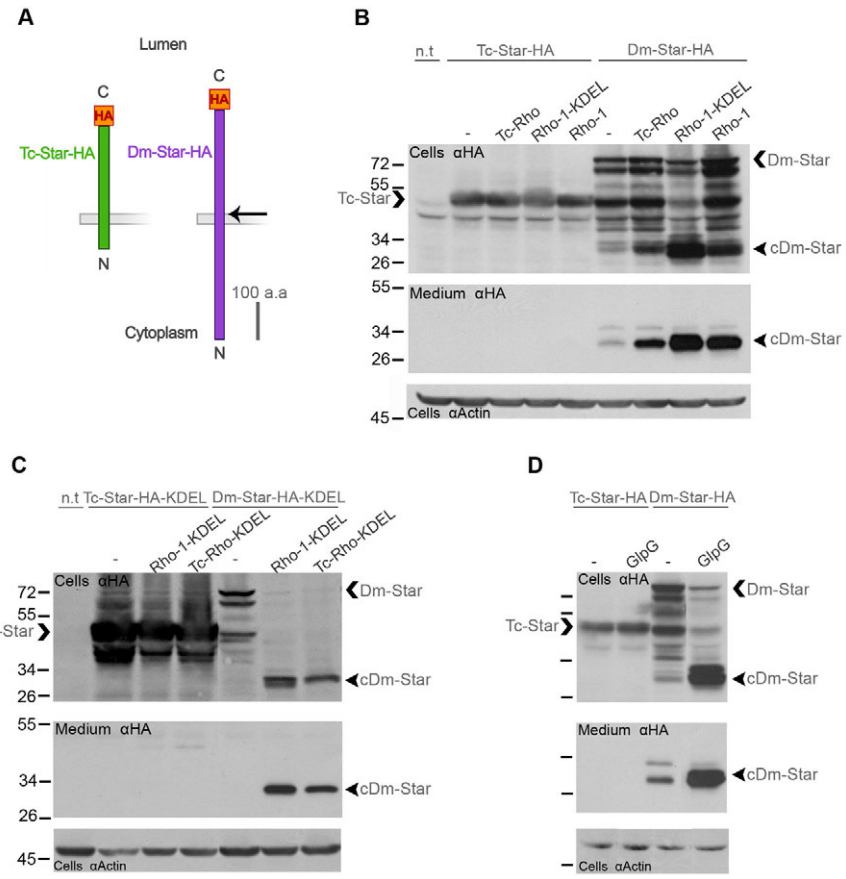

Fig. 3. Tc-Star is not cleaved by *Tribolium* or *Drosophila* Rhomboids. (**A**) Illustration of the C-terminally tagged Star constructs from the two species, drawn to scale. Arrow indicates cleavage site by Rhomboids in the vicinity of the transmembrane (TM) domain (Tsruya et al., 2007). (**B**) S2 cells were transfected with the indicated constructs, and cell lysates and media were probed with an anti-HA antibody and anti-Actin as a loading control. Following co-expression of Dm-Star-HA with different Rhomboids (right), a ~30 kDa cleaved form (cDm-Star, arrowhead) is detected in cells and cell medium, in addition to the 72 kDa full-length form (arrow). The cleaved fragment is detected at low levels in the absence of transfected Rhomboid, probably owing to low levels of endogenous Rhomboid in S2 cells. By contrast, only the ~50 kDa non-cleaved form of Tc-Star-HA (left, arrow) is detected following similar co-expression protocols. n.t, non-transfected. (**C**) Simultaneous targeting of both Star and Rhomboids to the ER by KDEL sequences results in the cleavage of Dm-Star-HA-KDEL (arrowheads) but not Tc-Star-HA-KDEL, as only the precursor is detected in the cells (arrow). (**D**) GlpG, the bacterial Rhomboid, cleaves Dm-Star (arrowhead) but not Tc-Star.

Rhomboids, cleaved forms of approximately the predicted size were detected in cell lysates and medium (Fig. 4C; see Fig. S4 in the supplementary material). Although readily detectable, cleavage of Bm-Star by the different Rhomboids tested is of intermediate efficiency, as judged by the abundance of full-length versus cleaved forms. Bm-Star might thus represent an intermediate stage in the evolution of Star cleavability.

The C-terminal domain of Star is crucial for cleavage by Rhomboids

The previous analyses established that properties of the Star protein are responsible for the differences in Star cleavability between species. A domain-swapping assay was undertaken to identify the critical domain for Star cleavage by Rhomboids. Swap constructs maintained their proper intracellular localization, as well as the capacity to traffic mSpi (see Fig. S5 in the supplementary material).

Transmembrane (TM) domains were exchanged between the *Tribolium* and *Drosophila* Star proteins, and Rhomboid-based cleavage of the complementary chimeras was followed in S2 cells. Swapping the TM domains between Dm-Star and Tc-Star did not alter the cleavage properties of the two proteins (Fig. 5C,E). Moreover, exchanging the TM domain of Dm-Star with that of an unrelated type II protein, the *Drosophila* TNF homolog Eiger (Moreno et al., 2002), did not compromise Dm-Star cleavage ability (Fig. 5D), strengthening the notion that the TM domain properties of Star do not influence cleavage. These conclusions also held when the Rhomboid compartment or source was modified (Fig. 5; see Fig. S5 in the supplementary material). Swapping the N-terminal cytosolic domain of Star between the two species revealed that it is not responsible for directing cleavage by Rhomboids (Fig. 5F,G).

Finally, a chimera that contains only the C-terminus from Dm-Star fused to the cytosolic and TM domains from Tc-Star was effectively cleaved by all Rhomboids tested (Fig. 5H; see Fig. S5 in the supplementary material). Conversely, Dm-Star that contained the C-terminal domain from Tc-Star did not undergo cleavage (Fig. 5I). We conclude that sequences within the luminal C-terminal domain of Dm-Star confer cleavability by Rhomboids.

Egfr ligand emanating from the *Tribolium* embryonic ventral midline triggers long-range activation

How do the distinct features of the *Tribolium* ligand-processing machinery impinge on Egfr-mediated signaling in *Tribolium* embryos? To address this issue, we chose to study patterning of the *Tribolium* embryonic ventral ectoderm. In *Tribolium* embryos, staining for dpERK, the active form of Egfr pathway component MAP kinase (MAPK), has revealed activation within the ventral ectoderm, emanating from the midline (Wheeler et al., 2005). This pattern is a hallmark of Egfr activation in *Drosophila* (Gabay et al., 1997), suggesting that Egfr activation in the ventral ectoderm of the embryo is conserved between the two species.

In situ hybridization assays for expression of the ligand-processing cassette (i.e. *Tc-tgfα*, *Tc-star*, *Tc-rho*) at the time of ventral ectoderm pattern formation suggested that they all play a role in Egfr activation (Fig. 6). *Tc-tgfα* was expressed in two broad ventrolateral stripes flanking the mesoderm (Fig. 6A). *Tc-star* was expressed weakly and uniformly, but showed some upregulation in the ventral ectoderm at the early germband stages (Fig. 6B) and was strongly elevated in the ventral midline during germband extension (Fig. 6C). Following the initiation of gastrulation and the

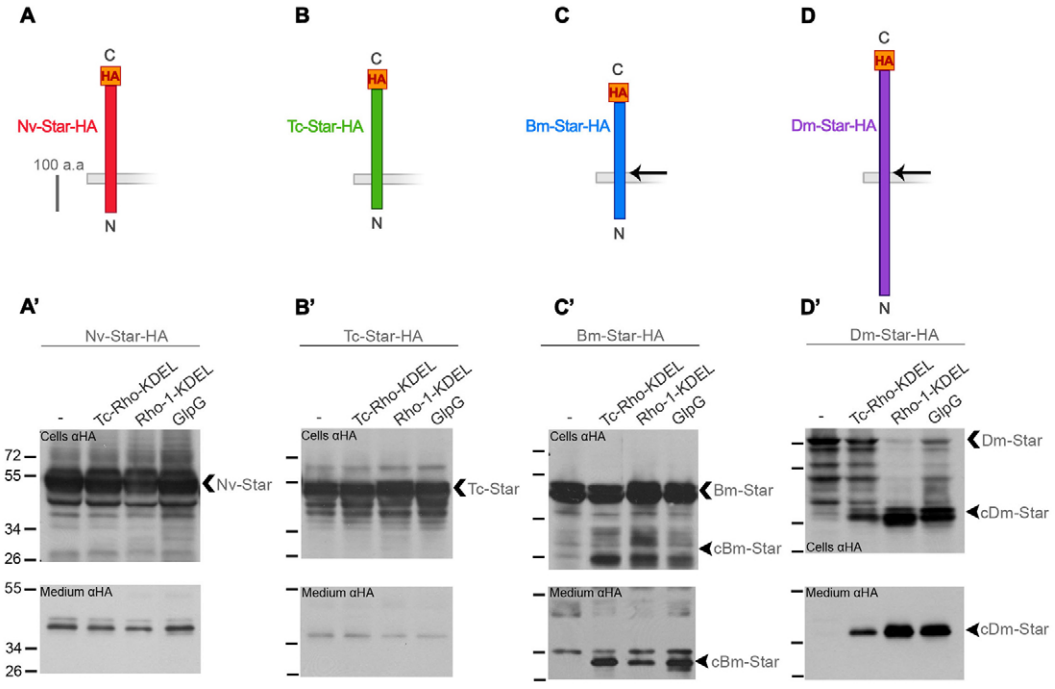

Fig. 4. Star cleavability in divergent insect species. (**A-D'**) Star proteins of divergent species were tested for cleavability in S2 cells. Schematic representations of the constructs used (A-D), to scale, are shown alongside the blots (A-D') for *Nasonia vitripennis* (Nv, A), *Tribolium castaneum* (Tc, B), *Bombyx mori* (Bm, C) and *Drosophila melanogaster* (Dm, D), according to the order of their phylogenetic relationship. Arrows indicate presumed cleavage site by Rhomboids. (A,B) Nv-Star-HA and Tc-Star-HA were not cleaved by any of the Rhomboids tested, as monitored in both cell lysates and medium. In the cells, only the full-length proteins were observed, at ~53 kDa and ~50 kDa, respectively (A',B', arrows). Non-specific bands are detected in the cell medium for both constructs, representing a cleavage event that is observed in the absence of transfected Rhomboid. (C) Bm-Star-HA was cleaved at intermediate efficiency by Rhomboids from distinct species, as indicated by the predicted ~28 kDa cleavage form detected in the medium (cBm-Star, arrowhead), below a non-specific cleavage form that is Rhomboid independent. Cleavage products are also detected in the cell lysates as a double band at ~23-30 kDa (C', arrowhead), in addition to the precursor form at ~47 kDa (C', arrow). (D) Cleavage of Dm-Star-HA is indicated by a ~37 kDa band in cells and medium (D', arrowheads).

formation of the germband, *Tc-rho* was prominently expressed in two broad ventrolateral stripes flanking the mesoderm (Fig. 6D). Later, during germband extension, the ectoderm fuses over the mesoderm progressively from anterior to posterior to form the ventral midline, the width of which can vary from one to three cells. *Tc-rho* was expressed in the midline cells (Fig. 6E). The restricted expression of Tc-Rho, similar to *rho-1* expression in *Drosophila* embryos (Golembo et al., 1996a), defines the cells that emit the processed Egfr ligand. The resulting dpERK pattern adjacent to the signal-producing cells allows monitoring of the range of the signal emanating from the midline. It is likely that this pattern faithfully reflects Egfr activation, in accordance with the expression pattern of the ligand-processing machinery and the similarity to the *Drosophila* ventral ectoderm.

We hypothesized that utilization of a non-cleavable Star in the context of an ER and secretory compartment Rhomboid, as found in *Tribolium*, should have implications for the signaling range of the ligand that triggers Egfr induction. The dpERK pattern extended several cell diameters from the *Tc-rho*-expressing cells, demonstrating long-range activation of the pathway in the ectoderm at both early and extending germband stages (Fig. 6D,E). This long-range activation pattern is similar to that in the *Drosophila* ventral ectoderm, where the signal emanating from the midline is considered to be the broadest among the tissues that are patterned by the Egfr pathway (Gabay et al., 1997). In *Drosophila* embryos, the long-range activation has been suggested to result from the exclusion of Rho-1 from the ER (Yogev et al., 2008), which prevents the encounter with Star in the ER. We suggest that because Tc-Star is refractive to cleavage by Rhomboid, the long-range Egfr activation in *Tribolium* reflects efficient intracellular ligand trafficking, despite the ER localization of Tc-Rho.

DISCUSSION

The fundamental features of the invertebrate Egfr ligand-processing cassette

The availability of a rudimentary Egfr ligand-processing cassette in *Tribolium*, with a single gene for each of the three major players, i.e. ligand, chaperone and protease, allowed us to identify the central hallmarks of the system that have been conserved during the ~300 million years of independent evolution separating *Drosophila* and *Tribolium*. We showed that most of the mechanistic features of the *Tribolium* system, such as trafficking of the ligand to a secretory compartment by Star, as well as recognition between all the components, can be demonstrated not only in cell culture but also in flies.

The single Egfr-associated *Tribolium* Rho appears to be most similar to Rho-2, both in terms of sequence and biological properties. When expressed in *Drosophila* cells or in flies, Tc-Rho exhibited dual localization to the ER and secretory compartment. Accordingly, Tc-Rho was able to trigger only low levels of Egfr activation when expressed in the wing disc.

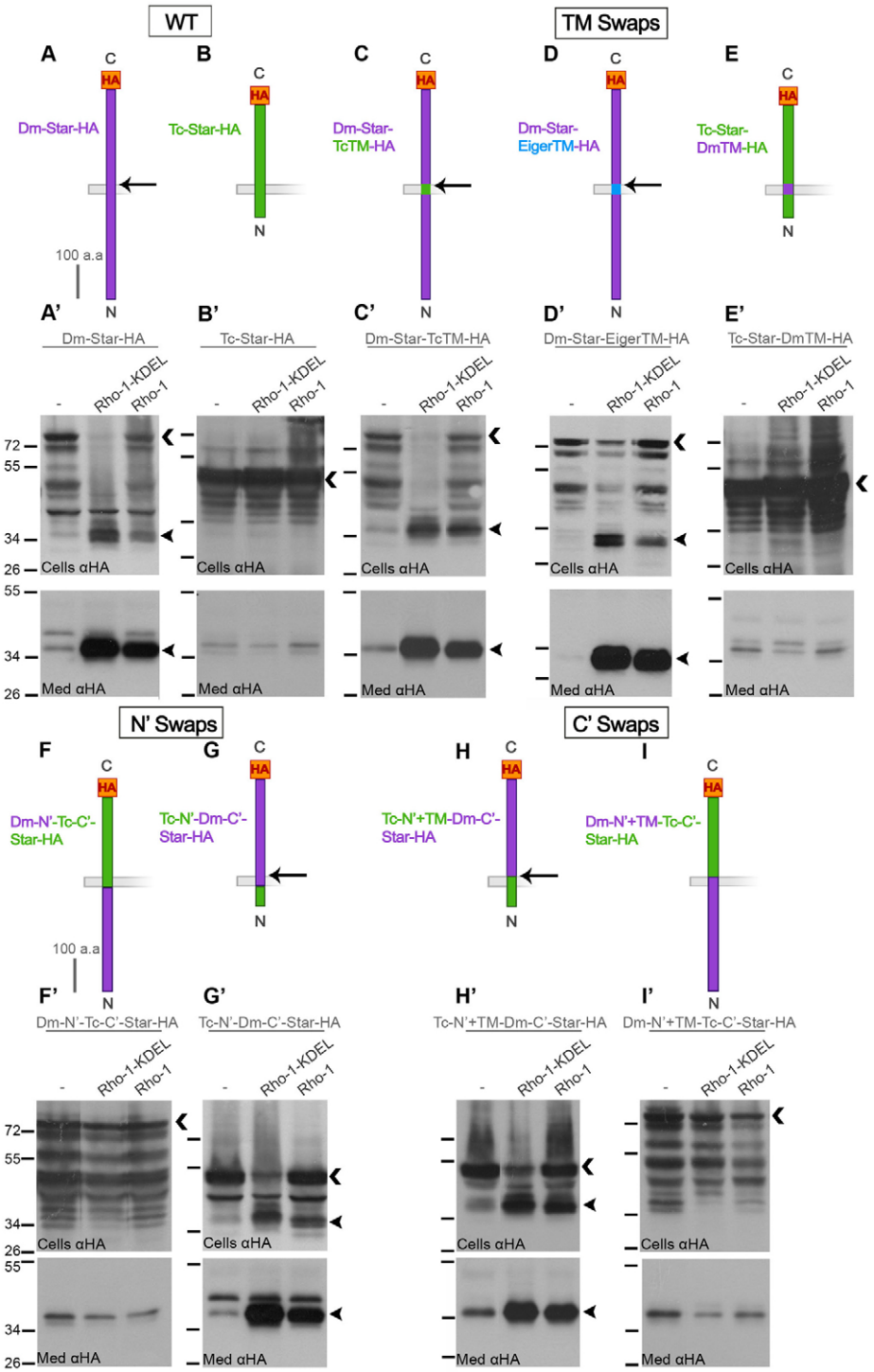

Fig. 5. The C-terminal luminal domain of Star directs cleavage by Rhomboids. (**A-B'**) Wild-type (WT) Dm-Star and Tc-Star constructs give rise to ~76 and ~50 kDa precursors, respectively (A',B', arrows). Following co-expression with Rhomboids, the cleavage form is detected for Dm-Star-HA (~37 kDa, arrowhead), but not for Tc-Star-HA for which only a Rhomboid-independent cleavage form is detected in the medium. (**C-E'**) TM domain swaps between Dm-Star and Tc-Star. The Dm-Star TM domain was replaced by that from Tc-Star (C, Dm-Star-TcTM-HA) or by that from another type II protein, Eiger (D, Dm-Star-EigerTM-HA). In both cases, cleavage was detected (C',D', arrowheads) in cells and medium, comparable to the cleavage of the wild-type Dm-Star. (E) Tc-Star containing the TM domain from Dm-Star (Tc-Star-DmTM-HA) showed no cleavage product in addition to the precursor at ~50 kDa (E', arrow). (**F-G'**) N-terminal swaps between *Drosophila* and *Tribolium* Star constructs. A Tc-Star construct with an N-terminal region from Dm-Star (F, Dm-N'-Tc-C'-Star-HA) is still not cleaved, as only the precursor is detected at ~74 kDa (F', arrow). (G) Co-expression of the reciprocal construct (Tc-N'-Dm-C'-Star-HA) with Rhomboids led to cleavage, as detected by a ~37 kDa form (G', arrowheads) in cells and medium, in addition to the ~54 kDa precursor in the cells (G', arrow). This cleavage is equivalent in efficiency to that of wild-type Dm-Star cleavage (A). (**H-I'**) C-terminal swaps between the *Drosophila* and *Tribolium* Star constructs. When the C-terminal domain from Dm-Star was inserted following Tc-Star N' and TM domains (H, Tc-N'+TM-Dm-C'-Star-HA) and co-expressed with Rhomboids, it was sufficient to mediate cleavage of this construct (H', arrowheads), as indicated by the appearance of a ~37 kDa band in cells and medium, in addition to the precursor construct at ~54 kDa. (I) The N' and TM domains of Dm-Star were not sufficient to confer cleavage to Tc-Star (I, Dm-N'+TM-Tc-C'-Star-HA), as only the precursor form of ~74 kDa was detected in the cells. Schematic representations of the different swap constructs, to scale, are shown above the blots. Arrows in A-I indicate presumed Rhomboid cleavage sites.

Divergence of Star cleavability by Rhomboids

In stark contrast to the conserved features of the ligand-processing cassette, the major difference we identified between the *Drosophila* and *Tribolium* systems is the accessibility of Star to cleavage by Rho proteases. Whereas Dm-Star is readily cleaved by Rho-1, Rho-2 and Rho-3 when brought into the same intracellular compartment, Tc-Star was not cleaved by *Tribolium* or *Drosophila* Rhomboids. What are the functional implications of the refractivity of Tc-Star to cleavage by Rho proteases? We suggest that despite colocalization of Tc-Rho and Tc-Star to the ER, Star remains intact and active. Tc-Star thus preserves the capacity to efficiently traffic the ligand to the secretory compartment, where the ligand is cleaved by Rhomboid and released from the cell. We predict, therefore, that the *Tribolium* cassette would give rise to high levels of processed ligand and long-range Egfr activation, despite the ER localization of Rhomboid.

The expression and activation features of the pathway in the ventral ectoderm of *Tribolium* embryos support this prediction. As dictated by the restricted expression of Tc-Rho, the active ligand should emanate from the midline to trigger Egfr in the adjacent ectodermal cells, similar to the paradigm in *Drosophila* (Golembo et al., 1996a). In the *Drosophila* embryo, signaling from the

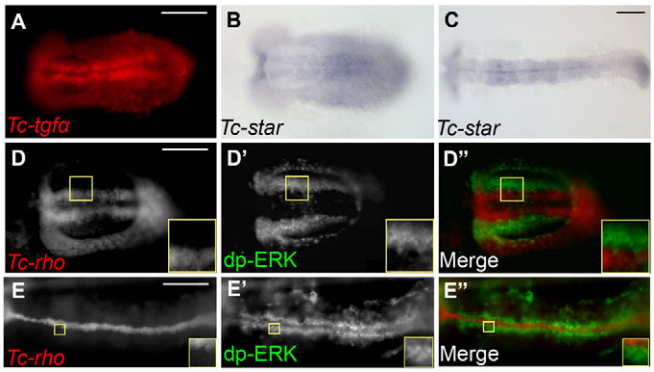

Fig. 6. The ligand-processing machinery in *Tribolium* embryos mediates long-range Egfr activation. (**A**) Expression of *Tc-tgfα* at the early germband stage (12-13 hours after egg laying). (**B**,**C**) Expression of *Tc-star* at the early (B) and extending (C,16-20 hours after egg laying) germband stages. (**D**,**E**) Expression of *Tc-rho* in early (D) and extending (E) germband stages. (**D′**,**E′**) Activation of Egfr signaling, as judged by the accumulation of dpERK. (**D″**,**E″**) Merge of *Tc-rho*-expressing cells and the adjacent dpERK-stained cells in the early (D″) and extending (E″) germband stages. In both stages, dpERK extends several cell diameters away from the *Tc-rho* expression domain, indicating long-range activation of Egfr signaling. dpERK staining is largely absent from the mesoderm and from the *Tc-rho*-expressing cells themselves. Scale bars: 100 μm

midline provides perhaps the longest signaling range of Egfr throughout development, and when monitored by dpERK antibodies, it has been shown to extend over four cell rows on each side (Gabay et al., 1997). By contrast, ectopic expression in *Drosophila* embryos of ER-localized Rho proteases, such as Rho-3, mediate activation levels that are significantly attenuated, as activation is detected only in the cells expressing the protease and never beyond (Yogev et al., 2008). In *Tribolium* embryos, the distribution of dpERK that was observed at the ventral ectoderm at both early and late stages was comparable to the dpERK distribution adjacent to the ventral midline of *Drosophila* embryos, indicating that high levels of processed Egfr ligand are indeed released from the midline cells. Interestingly, premature cleavage of the ligand by the activity of Rho in the ER does not seem to attenuate signaling in *Drosophila* (Yogev et al., 2008), possibly because the ligand precursor is produced in high excess or because the cleaved ligand can also be trafficked by Star from the ER. The observation of long-range Egfr activation in *Tribolium* triggered by an ER-localized Rhomboid suggests that ligand levels are also not limiting in this organism. Although it is formally possible that in *Tribolium* embryos the cleaved ligand produced in the ER would not be retained, and might undergo secretion in a chaperone-independent manner, we think this is unlikely in view of the striking structural and functional conservation of Star.

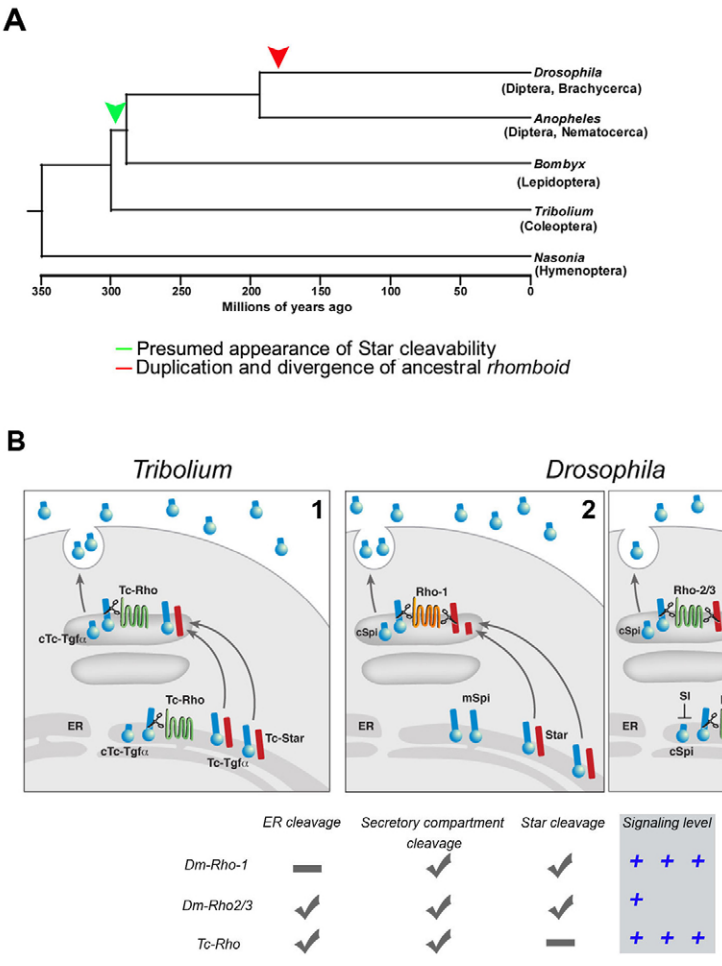

Fig. 7. Diversification of Egfr ligand processing during evolution. (**A**) Star cleavability and *rho* locus duplication in a phylogenetic context. Phylogenetic relationships and divergence times [see Wiegmann et al. (Wiegmann et al., 2009)]. The appearance of Star cleavability (green arrowhead) is hypothesized to have occurred after the divergence of the Coleoptera and the Diptera/Lepidoptera lineages, but before the divergence of the latter two orders. Based on analyses of sequenced insect genomes, the duplication and divergence of the ancestral *rho* gene, giving rise to *rho-1*, *rho-2* and *rho-3* in *Drosophila* (red arrowhead), probably took place in the Brachycercan lineage, after its divergence from the Nematocerca, as represented by *Anopheles gambi*. (**B**) Variations in the ligand-processing machinery generate distinct modes of Egfr signaling. In *Tribolium*, the single Rhomboid is active in the combined ER and secretory compartment mode (1). Signaling levels are high, however, because Tc-Star is refractive to Rhomboid cleavage in the ER. In *Drosophila*, multiple Rhomboids enable modulation of the signaling levels by differential compartmentalization. Rho-1 is distributed only to the secretory compartment and mediates high signaling levels (2). Rho-2 and Rho-3 employ the combined ER and secretory compartment cleavage, leading to an attenuated signal, primarily due to Star cleavage in the ER. The cleaved Spitz (cSpi) generated in the ER is retained by a Small wing (Sl)-dependent mechanism (Schlesinger et al., 2004) (3). The features and outcome of Egfr ligand processing in the two species are summarized beneath.

Mechanism of Star cleavage by Rhomboids

It is interesting to note that whereas the ligands cleaved by Rhomboids are all type I single transmembrane domain proteins, Star is a type II single transmembrane protein. The availability of orthologs of Star from other species, which display opposite behavior regarding cleavage by Rhomboids, might provide clues to the recognition of substrates by Rhomboids. The general notion is that the activity of Rhomboids is constitutive and that the different *Drosophila* Rhomboids possess the same substrate specificity when forced to the same compartment (Urban et al., 2002; Yogev et al., 2008). Interestingly, even the bacterial GlpG Rhomboid family member was able to cleave the *Drosophila* ligands and also Dm-Star (but not Tc-Star), highlighting the conserved substrate specificity.

When carrying out domain swaps between *Drosophila* and *Tribolium* Star, we found that the TM domain of Star appears to play a permissive role, as the TM domain from *Tribolium* allowed cleavage when used to replace the Dm-Star TM domain. Even insertion of a foreign type II TM domain from the Eiger protein into Dm-Star maintained cleavability by Rhomboids. These results imply that the structural basis for cleavage of Star by Rhomboids differs from the mechanism of cleavage of the type I TM family ligands, for which the crucial and perhaps single determinant is the sequence of the ligand TM domain (Urban et al., 2002).

Conversely, the extracellular domain of Star dictated cleavability of the protein. One possibility is that cleavage of Star by Rhomboids takes place immediately outside the TM domain, as has been demonstrated for some Rhomboid substrates (Strisovsky et al., 2009). Since Star is a type II transmembrane protein, in contrast to all other Rhomboid substrates, a Star substrate recognition motif outside of the TM domain might allow the protein to loop back and display a motif similar in orientation to that of type I proteins. Alternatively, the extracellular domain of Star might mediate an interaction with Rhomboid that is distinct from substrate recognition. For some Rhomboid substrates, such as Thrombomodulin, sequences outside the TM domain have been shown to be crucial for recognition and cleavage (Lohi et al., 2004).

Elaboration of the Egfr ligand-processing cassette during insect evolution

By sampling representatives of four major lineages of the Holometabola, we have the opportunity to hypothesize as to the evolutionary history of the Egfr ligand-processing cassette in holometabolous insects. It is likely that the ancestral cassette contained a single Rhomboid, as this state is found in all insects whose genomes have been sequenced, except *Drosophila* (Fig. 7A). This single Rhomboid was likely to have been targeted to both ER and secretory compartments, as this is what is found for the single *Tribolium* Rhomboid. Regarding Star evolution, the most parsimonious hypothesis is that it was ancestrally uncleavable by Rho, as this is the state found in the two most basally branching taxa examined, *Nasonia* and *Tribolium*.

With these ancestral characters mapped on the phylogeny, we can outline the process that generated the novel characteristics of the *Drosophila* Egfr ligand-processing cassette. It is clear that one evolutionary change entailed duplications of the *rho* gene so as to generate multiple *rho* paralogs in *Drosophila* (*rho-1*, *rho-2* and *rho-3*), each under a different set of transcriptional regulators. In addition, the paralog encoding Rho-1 has undergone structural changes in its coding sequence that have eliminated the localization of Rho-1 to the ER. Star cleavability might have originated in a common ancestor of *Bombyx* and *Drosophila*, and was further elaborated in the lineage leading to *Drosophila* (Fig. 7A).

The rudimentary ligand-processing cassette analyzed in *Tribolium* gives rise to a single signaling mode, characterized by high levels of secreted ligand (Fig. 7B). In *Drosophila*, the combination of cleavable Star and diversity of Rhomboid localization generates two modes of ligand processing (Fig. 7B). These two modalities induce different ranges of Egfr activation in distinct tissues, allowing a more elaborate and diversified utilization of the pathway.

Acknowledgements

We thank R. Tsruya for generating the Dm-Star-EigerTM construct; the Developmental Studies Hybridoma Bank for antibodies; and all members of the B.-Z.S. laboratory for criticism and support throughout the project. The work was funded by the US-Israel BSF grant to B.-Z.S., who is an incumbent of the Hilda and Cecil Lewis Chair in Molecular Genetics.

Competing interests statement

The authors declare no competing financial interests.

Supplementary material

Supplementary material for this article is available at http://dev.biologists.org/lookup/suppl/doi:10.1242/dev.049858/-/DC1

References

Blobel, C. P., Carpenter, G. and Freeman, M. (2009). The role of protease activity in ErbB biology. *Exp. Cell Res.* **315**, 671-682.

Casci, T., Vinos, J. and Freeman, M. (1999). Sprouty, an intracellular inhibitor of Ras signaling. *Cell* **96**, 655-665.

Gabay, L., Seger, R. and Shilo, B. Z. (1997). In situ activation pattern of Drosophila EGF receptor pathway during development. *Science* **277**, 1103-1106.

Ghiglione, C., Amundadottir, L., Andresdottir, M., Bilder, D., Diamonti, J. A., Noselli, S., Perrimon, N. and Carraway, I. K. (2003). Mechanism of inhibition of the Drosophila and mammalian EGF receptors by the transmembrane protein Kekkon 1. *Development* **130**, 4483-4493.

Golembo, M., Raz, E. and Shilo, B. Z. (1996a). The Drosophila embryonic midline is the site of Spitz processing, and induces activation of the EGF receptor in the ventral ectoderm. *Development* **122**, 3363-3370.

Golembo, M., Schweitzer, R., Freeman, M. and Shilo, B. Z. (1996b). Argos transcription is induced by the Drosophila EGF receptor pathway to form an inhibitory feedback loop. *Development* **122**, 223-230.

Guichard, A., Roark, M., Ronshaugen, M. and Bier, E. (2000). brother of rhomboid, a rhomboid-related gene expressed during early Drosophila oogenesis, promotes EGF-R/MAPK signaling. *Dev. Biol.* **226**, 255-266.

Kramer, S., Okabe, M., Hacohen, N., Krasnow, M. A. and Hiromi, Y. (1999). Sprouty: a common antagonist of FGF and EGF signaling pathways in Drosophila. *Development* **126**, 2515-2525.

Lee, J. R., Urban, S., Garvey, C. F. and Freeman, M. (2001). Regulated intracellular ligand transport and proteolysis control EGF signal activation in Drosophila. *Cell* **107**, 161-171.

Lohi, O., Urban, S. and Freeman, M. (2004). Diverse substrate recognition mechanisms for rhomboids; thrombomodulin is cleaved by Mammalian rhomboids. *Curr. Biol.* **14**, 236-241.

Markstein, M., Pitsouli, C., Villalta, C., Celniker, S. E. and Perrimon, N. (2008). Exploiting position effects and the gypsy retrovirus insulator to engineer precisely expressed transgenes. *Nat. Genet.* **40**, 476-483.

Mazzoni, E. O., Celik, A., Wernet, M. F., Vasiliauskas, D., Johnston, R. J., Cook, T. A., Pichaud, F. and Desplan, C. (2008). Iroquois complex genes induce co-expression of rhodopsins in Drosophila. *PLoS Biol.* **6**, e97.

Moreno, E., Yan, M. and Basler, K. (2002). Evolution of TNF signaling mechanisms: JNK-dependent apoptosis triggered by Eiger, the Drosophila homolog of the TNF superfamily. *Curr. Biol.* **12**, 1263-1268.

Reich, A., Sapir, A. and Shilo, B. (1999). Sprouty is a general inhibitor of receptor tyrosine kinase signaling. *Development* **126**, 4139-4147.

Richards, S., Gibbs, R. A., Weinstock, G. M., Brown, S. J., Denell, R., Beeman, R. W., Gibbs, R., Bucher, G., Friedrich, M., Grimmelikhuijzen, C. J. et al. (2008). The genome of the model beetle and pest Tribolium castaneum. *Nature* **452**, 949-955.

Schlesinger, A., Kiger, A., Perrimon, N. and Shilo, B. Z. (2004). Small Wing PLCgamma is required for ER retention of cleaved spitz during eye development in Drosophila. *Dev. Cell* **7**, 535-545.

Schulz, C., Wood, C. G., Jones, D. L., Tazuke, S. I. and Fuller, M. T. (2002). Signaling from germ cells mediated by the rhomboid homolog stet organizes encapsulation by somatic support cells. *Development* **129**, 4523-4534.
Shilo, B. Z. (2003). Signaling by the Drosophila epidermal growth factor receptor pathway during development. *Exp. Cell Res.* **284**, 140-149.
Shilo, B. Z. (2005). Regulating the dynamics of EGF receptor signaling in space and time. *Development* **132**, 4017-4027.
Strisovsky, S., Sharpe, H. J. and Freeman, M. (2009). Sequence-specific intramembrane proteolysis: identification of a recognition motif in Rhomboid substrates. *Mol. Cell* **36**, 1048-1059.
Sturtevant, M. A., Roark, M. and Bier, E. (1993). The Drosophila rhomboid gene mediates the localized formation of wing veins and interacts genetically with components of the EGF-R signaling pathway. *Genes Dev.* **7**, 961-973.
Tautz, D. and Pfeifle, C. (1989). A non-radioactive in situ hybridization method for the localization of specific RNAs in Drosophila embryos reveals translational control of the segmentation gene hunchback. *Chromosoma* **98**, 81-85.
Tsruya, R., Schlesinger, A., Reich, A., Gabay, L., Sapir, A. and Shilo, B. Z. (2002). Intracellular trafficking by Star regulates cleavage of the Drosophila EGF receptor ligand Spitz. *Genes Dev.* **16**, 222-234.
Tsruya, R., Wojtalla, A., Carmon, S., Yogev, S., Reich, A., Bibi, E., Merdes, G., Schejter, E. and Shilo, B. Z. (2007). Rhomboid cleaves Star to regulate the levels of secreted Spitz. *EMBO J.* **26**, 1211-1220.
Urban, S., Lee, J. R. and Freeman, M. (2001). Drosophila rhomboid-1 defines a family of putative intramembrane serine proteases. *Cell* **107**, 173-182.
Urban, S., Lee, J. R. and Freeman, M. (2002). A family of Rhomboid intramembrane proteases activates all Drosophila membrane-tethered EGF ligands. *EMBO J.* **21**, 4277-4286.
Wasserman, J. D., Urban, S. and Freeman, M. (2000). A family of rhomboid-like genes: Drosophila rhomboid-1 and roughoid/rhomboid-3 cooperate to activate EGF receptor signaling. *Genes Dev.* **14**, 1651-1663.
Wheeler, S. R., Carrico, M. L., Wilson, B. A. and Skeath, J. B. (2005). The Tribolium columnar genes reveal conservation and plasticity in neural precursor patterning along the embryonic dorsal-ventral axis. *Dev. Biol.* **279**, 491-500.
Wiegmann, B. M., Trautwein, M. D., Kim, J. W., Cassel, B. K., Bertone, M. A., Winterton, S. L. and Yeates, D. K. (2009). Single-copy nuclear genes resolve the phylogeny of the holometabolous insects. *BMC Biol.* **7**, 34.
Yogev, S., Schejter, E. D. and Shilo, B. Z. (2008). Drosophila EGFR signalling is modulated by differential compartmentalization of Rhomboid intramembrane proteases. *EMBO J.* **27**, 1219-1230.

Figure S1A

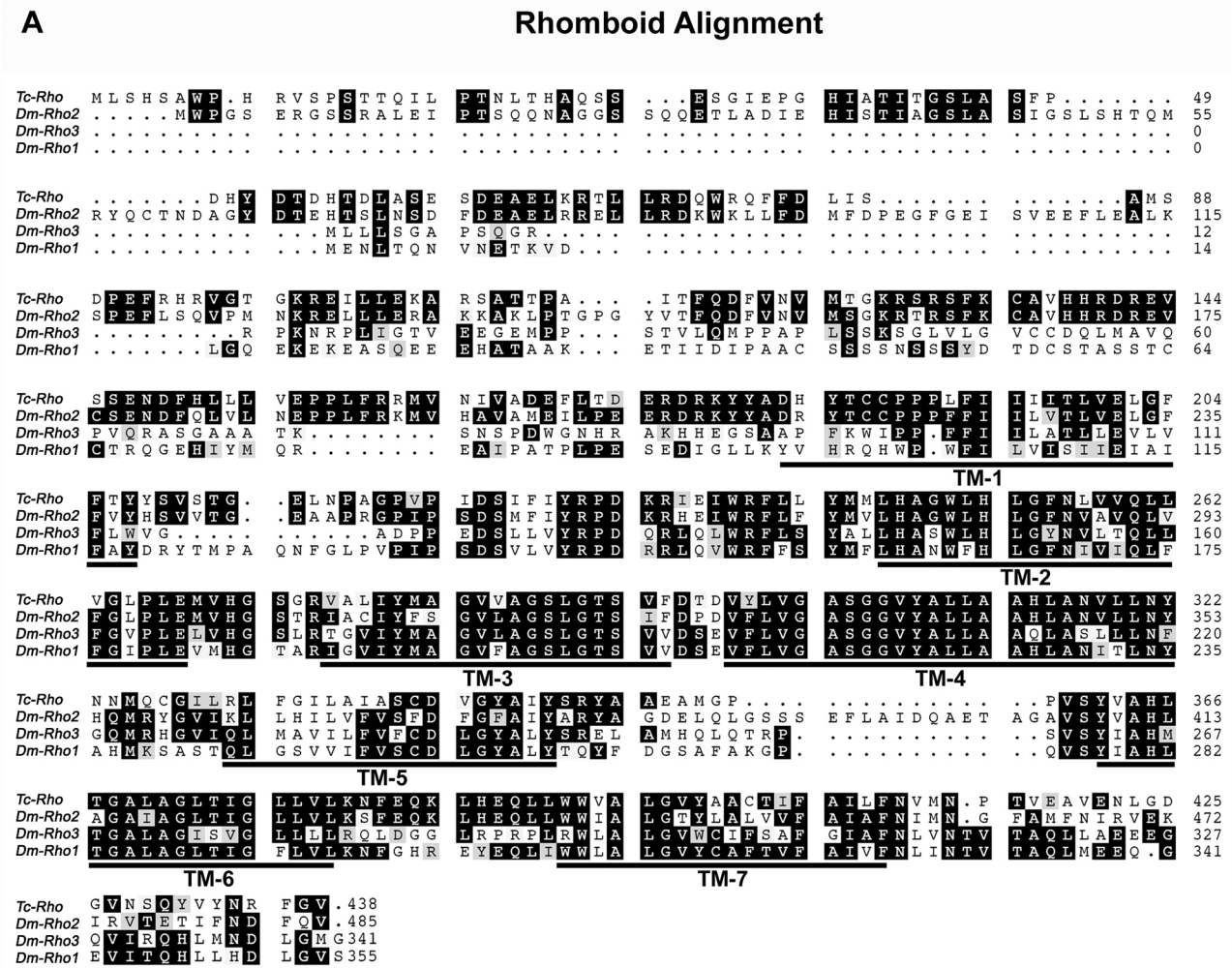
A
Rhomboid Alignment
Tc-Rho
Dm-Rho2
Dm-Rho3
Dm-Rho1
TM-1
TM-2
TM-3
TM-4
TM-5
TM-6
TM-7

Figure S1B-C

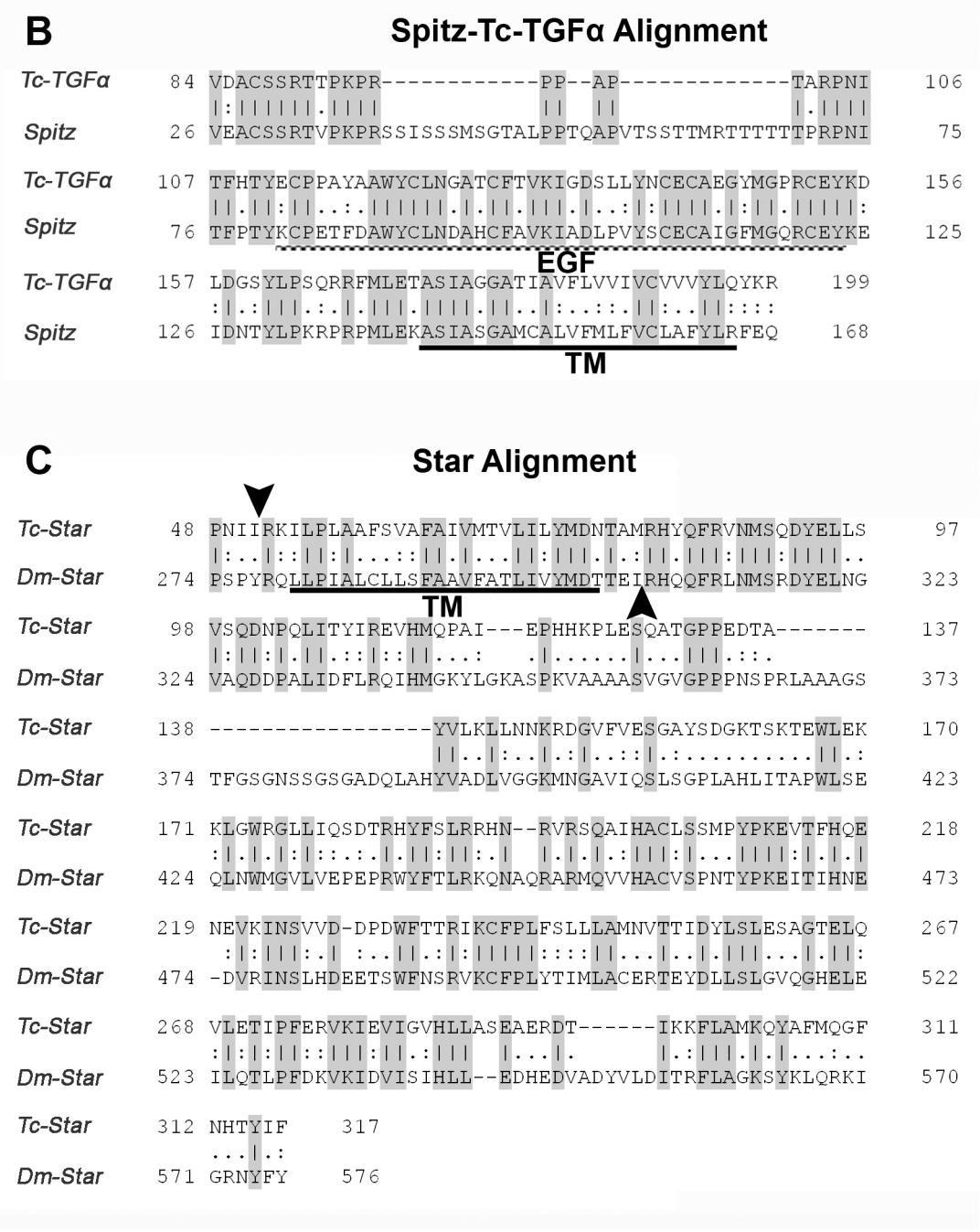
B
Spitz-Tc-TGFα Alignment
Tc-TGFα 84 VDACSSRTTPKPR----------PP--AP----------TARPNI 106
Spitz 26 VEACSSRTVPKPRSSISSSMSGTALPPTQAPVTSSTTMRTTTTTTPRPNI 75
Tc-TGFα 107 TFHTYECPPAYAAWYCLNGATCFTVKIGDSLLYNCECAEGYMGPRCEYKD 156
Spitz 76 TFPTYKCPETFDAWYCLNDAHCFAVKIADLPVYSCECAIGFMGQRCEYKE 125
EGF
Tc-TGFα 157 LDGSYLPSQRRFMLETASIAGGATIAVFLVVIVCVVVYLQYKR 199
Spitz 126 IDNTYLPKRPRPMLEKASIASGAMCALVFMLFVCLAFYLRFEQ 168
TM
C
Star Alignment
Tc-Star 48 PNIIRKILPLAAFSVAFAIVMTVLILYMDNTAMRHYQFRVNMSQDYELLS 97
Dm-Star 274 PSPYRQLLPIALCLLSFAAVFATLIVYMDTTEIRHQQFRLNMSRDYELNG 323
TM
Tc-Star 98 VSQDNPQLITYIREVHMQPAI---EPHHKPLESQATGPPEDTA------- 137
Dm-Star 324 VAQDDPALIDFLRQIHMGKYLGKASPKVAAAASVGVGPPPNSPRLAAAGS 373
Tc-Star 138 ----------YVLKLLNNKRDGVFVESGAYSDGKTSKTEWLEK 170
Dm-Star 374 TFGSGNSSGSGADQLAHYVADLVGGKMNGAVIQSLSGPLAHLITAPWLSE 423
Tc-Star 171 KLGWRGLLIQSDTRHYFSLRRHN--RVRSQAIHACLSSMPYPKEVTFHQE 218
Dm-Star 424 QLNWMGVLVEPEPRWYFTLRKQNAQRARMQVVHACVSPNTYPKEITIHNE 473
Tc-Star 219 NEVKINSVVD-DPDWFTTRIKCFPLFSLLLAMNVTTIDYLSLESAGTELQ 267
Dm-Star 474 -DVRINSLHDEETSWFNSRVKCFPLYTIMLACERTEYDLLSLGVQGHELE 522
Tc-Star 268 VLETIPFERVKIEVIGVHLLASEAERDT------IKKFLAMKQYAFMQGF 311
Dm-Star 523 ILQTLPFDKVKIDVISIHLL--EDHEDVADYVLDITRFLAGKSYKLQRKI 570
Tc-Star 312 NHTYIF 317
Dm-Star 571 GRNYFY 576

Figure S1D

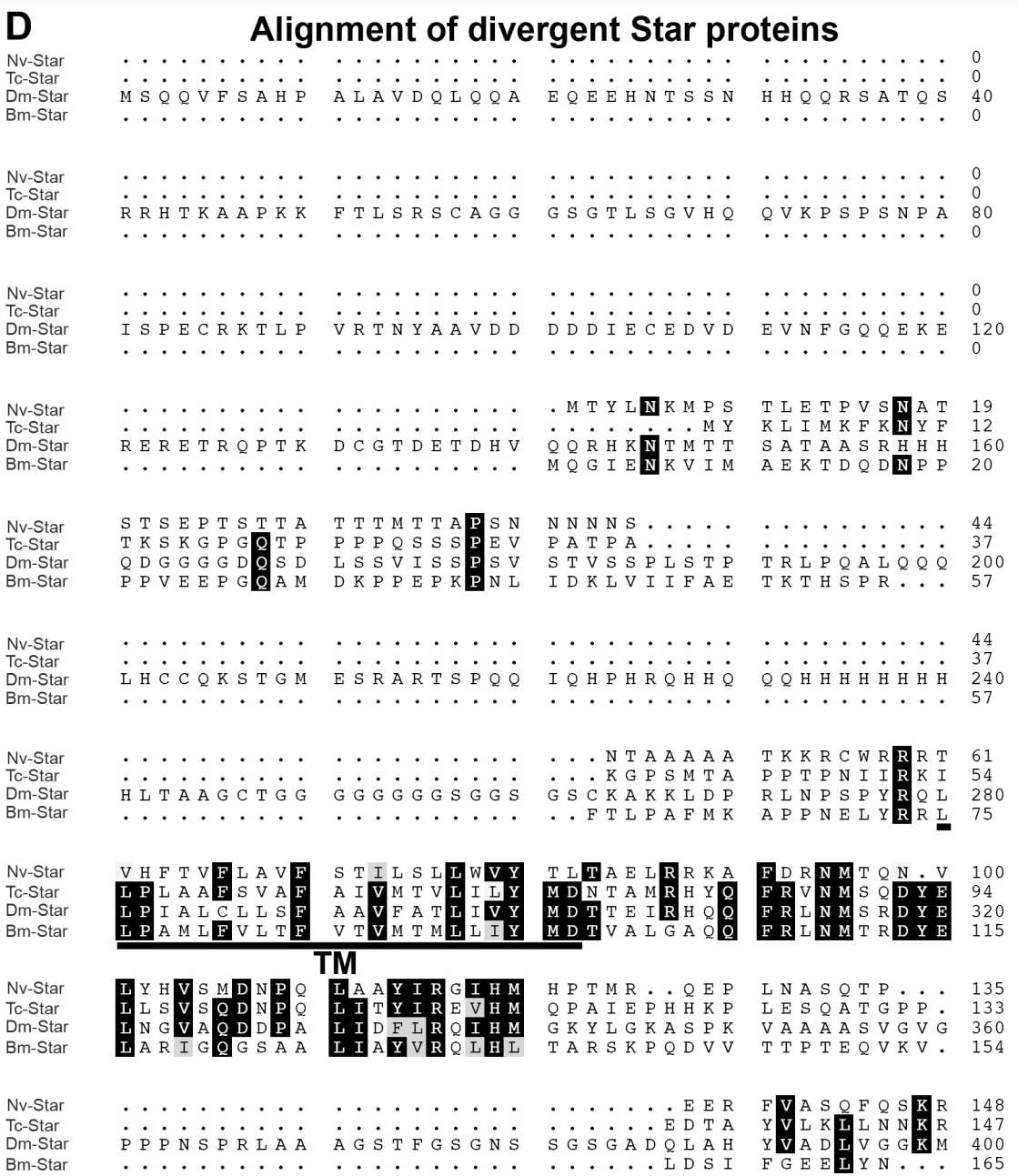
D
Alignment of divergent Star proteins
Nv-Star
Tc-Star
Dm-Star
Bm-Star
TM

Figure S1D-Continued